Journal of Thermal Analysis, Vol. 42 (1994) 307-330

HEAT CAPACITY MEASUREMENT BY MODULATED DSC AT CONSTANT TEMPERATURE *

A. Boller, Y. Jin and B. Wunderlich

Department of Chemistry, University of Tennessee, Knoxville, TN 37996 and Chemistry and Analytical Science Division, Oak Ridge National Laboratory, Oak Ridge, TN 37831, USA

Abstract

The mathematical equations for step-wise measurement of heat capacity (C_p) by modulated differential scanning calorimetry (MDSC) are discussed for the conditions of negligible temperature gradients within sample and reference. Using a commercial MDSC, applications are evaluated and the limits explored. This new technique permits the determination of C_p by keeping the sample continually close to equilibrium, a condition conventional DSC is unable to meet. Heat capacity is measured at 'practically isothermal condition' (often changing not more than ±1 K). The method provides data with good precision. The effects of sample mass, amplitude and frequency of temperature modulation were studied and methods for optimizing the instrument are proposed. The correction for the differences in sample and reference heating rates, needed for high-precision data by standard DSC, do not apply for this method.

Keywords: heat capacity, modulated DSC

* Presented in preliminary from at the 22nd NATAS Conference in Denver, CO 9/19–22/93 (Proceedings, pages 59–64, editor K. R. Williams).

0368–4466/94/ $ 4.00

John Wiley & Sons, Limited
Chichester

Introduction

Heat capacity (C_p) is one of the basic properties of a material. The improvement of C_p measurements by differential scanning calorimetry (DSC) is one of the goals in our Advanced THermal AnalysiS laboratory (ATHAS). In the past, comparisons between various differential scanning calorimeters were made in high [1] and low temperature ranges [2], direct computerization was pioneered [3], and a new single-run C_p measurement was proposed [4] and tested using the Dual Sample DSC of TA Instruments [5–7].

Recently, a novel, modulated DSC has been commercialized [8]. One of the new features of this system is the ability to measure heat capacity directly, using slow heating rates or even quasi-isothermal conditions. A more detailed description of the mathematical background of the instrument was prepared by us [9]. General applications have been presented in the literature [10]. In this paper, quasi-isothermal MDSC is discussed and tests are described that set the experimental boundaries of this technique.

Calorimeters based on periodic heating are known for some times as AC calorimeters [11]. Even a differential AC calorimeter has been proposed [12]. Only few heat capacities have been measured utilizing these methods. Furthermore, most of the data reported at temperatures above about 100 K did not have sufficient quality to be included in our critically reviewed data bank of heat capacities of macromolecules. The main reasons for the failure of these attempts at measurement of heat capacity using AC calorimetry have been limited control of heating and cooling, poor design of the calorimeter proper, and insufficient data collection and calibration. In the present calorimeter a standard DSC, already proven to be able to measure heat capacity with good precision using a controlled, linear heating rate [1, 2], is modulated to improve the control of the main experimental uncertainty, the heat loss [13–16]. The heat losses are naturally not occurring with the modulation frequency and can thus be eliminated by proper data treatment. In this more detailed analysis of MDSC, we chose the quasi-isothermal operation mode to reach highest precision for the measurement of heat capacity. By adding a constant heating rate to the here described isothermal experiments, additional normal DSC results can be obtained by proper data treatment. These combined analyses produce a reversing signal (measured by MDSC) and a nonreversing signal (difference of the standard, total DSC heat flow signal and the modulation-caused signal). Especially for macromolecules this method is then able to give additional insight into nonequilibrium processes occurring during the glass transition (strain release, shrinkage, etc.) and during crystallization and melting (crystal perfection, recrystallization, softening of rigid amorphous content, etc.). Work on the latter topics is in progress and will be presented in due time [17].

Principle of the measurement

Unlike the conventional DSC that operates with linear heating or cooling rates q, modulated DSC adds a sinusoidal oscillation to the experiment. If the instrument has reached steady state, the block, sample and reference temperatures T_b, T_s and T_r, respectively, at time t, are [9]:

$$T_b(t) = T_0 + qt + A_{T_b}\sin(\omega t) \tag{1}$$

$$T_s(t) = T_0 + qt - \frac{qC_s}{K} + A_{T_s}\sin(\omega t - \varepsilon) \tag{2}$$

$$T_r(t) = T_0 + qt - \frac{qC_r}{K} + A_{T_r}\sin(\omega t - \varphi) \tag{3}$$

where T_0 is the initial temperature, q, the underlying linear heating rate (= zero in the applications discussed in this paper), and the A_T designate the corresponding oscillation amplitudes (subscripts b = block, s = sample, and r = reference). The frequency of oscillation is $\omega = 2\pi/p$, with p being the period in s (or minutes). The sample and reference heat capacities are C_s and C_r

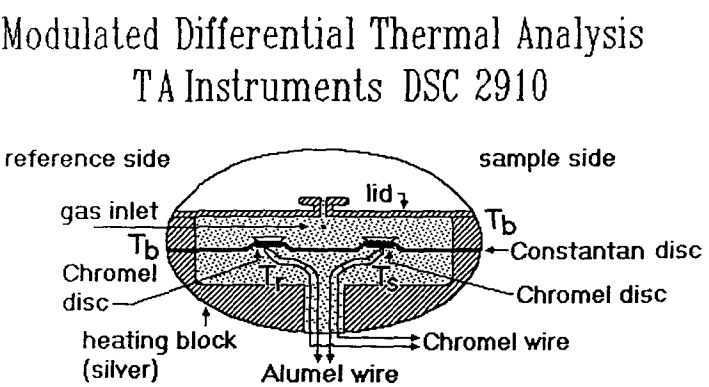

Normalized, phase-shifted temperatures for isothermal MDSC:

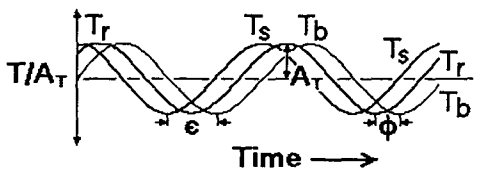

Fig. 1 Schematic of the MDSC and normalized temperature *vs.* time plots. (By dividing the respective values of T by their corresponding A_T, T_b, T_s and T_r have the same amplitudes. Note that T_b is not recorded in the equipment used.)

and K is the Newton's law constant [$J \cdot s^{-1} \cdot K^{-1}$]. Figure 1 illustrates the schematic of the calorimeter and the temperatures, normalized to equal maximum amplitudes and for the case that $q = 0$, the case of importance for this paper. The actual, oscillating heating and cooling rates of the sample at any given time can then be described as follows:

$$\frac{dT_s}{dt} = A_{T_s}\,\omega\cos(\omega t - \varepsilon) = A_{HR}\cos(\omega t - \varepsilon) \tag{4}$$

where A_{HR} is the amplitude of the heating rate oscillation.

As is well known, the heat capacity C_p, measured with the standard, not oscillating heat-conduction DSC with linear heating or cooling and under the condition of negligible temperature gradient within the sample can be expressed as follows [13, 14]:

$$C_p = K\Delta T / q + [(C' + K\Delta T / q)(d\Delta T / dT_s)] \tag{5}$$

where ΔT is the temperature difference between reference and sample, K is the temperature-dependent Newton's law constant, determined by heat capacity comparison with a calibration standard like sapphire (Al_2O_3) [18], and C' is the heat capacity of the empty reference pan (equal weight reference and sample pans are assumed, and as usual, perfect symmetry of the DSC so that reference and sample side can use the same K). The term in brackets is small for C_p measurements (about 1%) and often omitted. The heat capacity is then, however, only approximately proportional to the temperature difference between sample and reference or heat flow measured by DSC:

$$C_p = K\Delta T / q = K'\Delta HF / q \tag{6}$$

where ΔHF is the differential heat flow into or out of sample and reference (usually in mW), diminished by the heat flow for a run with empty sample and reference pans (baseline); K' is the appropriately changed calibration constant when recording heat flow instead of the temperature difference (K' is dimensionless). Both, ΔT and ΔHF are proportional to q.

In order to get high precision heat capacity by standard DSC, one must have a high enough heating rate q to get a large ΔT and ΔHF, and the corrections suggested by Eq. (5) must be made. In typical, present-day DSC, the lower limit for q is about 5 deg·min^{-1}. Often rates as high as 40 deg·min^{-1} are used to increase precision, but such fast heating rates reach the limit of operation with minimal temperature lag within the sample. The quasi-isothermal MDSC permits measurement with $q = 0$ in Eq. (1). This leads for the first time in scanning calorimetry based on heat conduction, to a true representation of heat

capacity since there is no need to correct for the differences in heating rates of reference and sample. Furthermore, the oscillating mode rejects drifts of the calorimeter that are not oscillating with the same frequency ω. The disadvantage of the slow generation of data points (one per run at T_0) is easily overcome by automatically stepping through a series of different temperatures. In this fashion some 10 points can be generated per h. Leaving the heat capacity mode for night-time, automatic operation of the instrument permits data generation at a rate of one sample per night, some 200 a year and leaves the instrument for the more routine operation during the day. At this rate a single MDSC could in one year double the number of heat capacity measurements published on polymers over the last 50 years (and summarized in the ATHAS data bank).

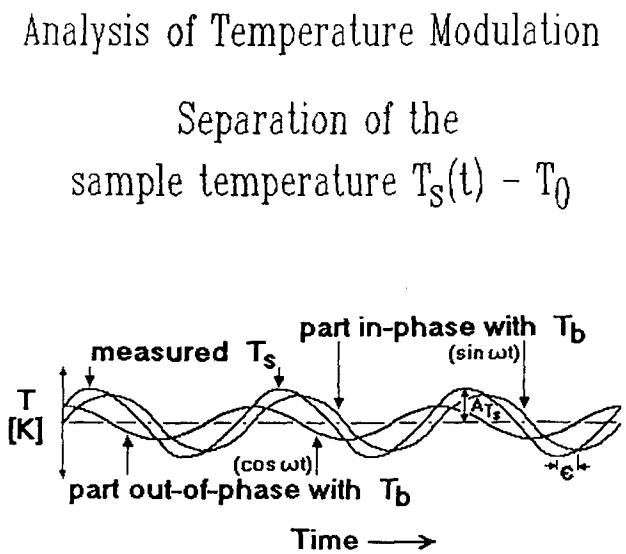

Fig. 2 Separation of the sample temperature into components in-phase and out-of-phase with the block temperature T_b (Fig. 1)

Derivation of the equations for quasi-isothermal heat capacity measurement

The oscillating temperatures under quasi-isothermal conditions ($q = 0$ and $T_0 =$ constant) are shown in Fig. 1. In Fig. 2 the separation of T_s into one part in-phase with the modulated block temperature T_b [Eq. (1)] and the other out-of-phase is illustrated. Mathematically this can be expressed by:

$$T_s(t) - T_0 = A_{T_s}\sin(\omega t - \varepsilon) = A_{T_s}[\cos\varepsilon \sin\omega t - \sin\varepsilon \cos\omega t] \quad (7)$$

Equation (7) is based on the addition theorem of trigonometric functions that is written as $\sin(\alpha-\beta) = \cos\beta \sin\alpha - \sin\beta \cos\alpha$. The first component of $T_s(t)-T_0$ is in-phase with the block temperature T_b, the second, out-of-phase. One can also represent the two components in a complex plane, recognizing that $\sin\theta - i\cos\theta = -ie^{i\theta}$:

$$T_s(t) - T_0 = A_{T_s}\, ie^{i(\omega t - \varepsilon)} \tag{8}$$

The more common representation $\cos\theta + i\sin\theta = e^{i\theta}$ differs from the here used expression by a phase shift of $\pi/2$, necessary since the initial condition, at time zero, is $T_s = T_r = T_b = T_0$ and $\Delta T = 0$. The temperature difference $\Delta T = T_r - T_s$ can be derived from Eqs (2) and (3). In complex notation ΔT is:

$$T_r - T_s = \Delta T = A_\Delta\, ie^{i(\omega t - \delta)} \tag{9}$$

with the phase angle $\delta = \varepsilon - \varphi$ and the maximum amplitude T_Δ.

Newton's law of cooling can be written as [14]:

$$\frac{dQ}{dt} = K[T_b - T] \tag{10}$$

Next, Eq. (10) can be used to find expressions for the sample and reference heat capacities C_s and C_r, by insertion of $Q = C_p[T-T_0]$. Assuming that C_p is constant over the full oscillation one can derive that:*

$$T_r - T_s = \frac{(C_s - C_r)}{K}\frac{dT_s}{dt} - \frac{C_r}{K}\frac{d(T_r - T_s)}{dt} \tag{11}$$

Inserting Eqs (8) and (9) into Eq. (11) yields:

$$A_\Delta\, e^{i(\omega t - \delta)} = \frac{(C_s - C_r)}{K} A_{T_s}\, i\omega e^{i(\omega t - \varepsilon)} - \frac{C_r}{K} A_\Delta\, i\omega e^{i(\omega t - \delta)} \tag{12}$$

that can be solved as:

$$e^{-i(\varepsilon - \delta)} = -\frac{KA_\Delta i}{A_{T_s}\omega(C_s - C_r)} + \frac{A_\Delta C_r}{A_{T_s}(C_s - C_r)} \tag{13}$$

* $KC_s[dT_s/dt] = T_b - T_s$; $KC_r[dT_r/dt] = T_b - T_r$ as derived in Fig. 4.17 of [14] gives the equation as written by taking the appropriate difference and adding and subtracting $(C_r/K)/(dT_r/dt)$

By equating the imaginary and the real parts on both sides of Eq. (13), one finds:

$$\sin(\varepsilon - \delta) = \frac{KA_\Delta}{A_{T_s}\omega(C_s - C_r)} \tag{14}$$

$$\cos(\varepsilon - \delta) = \frac{A_\Delta C_r}{A_{T_s}(C_s - C_r)} \tag{15}$$

Equations (14) and (15) can be combined by remembering that $\sin^2\theta + \cos^2\theta = 1$:

$$1 = \left(\frac{KA_\Delta}{A_{T_s}\omega(C_s - C_r)}\right)^2 + \left(\frac{A_\Delta C_r}{A_{T_s}(C_s - C_r)}\right)^2 \tag{16}$$

Equation (16) can be changed to an equation for the heat capacity:

$$(C_s - C_r) = A_\Delta / A_{T_s}\sqrt{(K/\omega)^2 + C_r^2} \tag{17}$$

Equation (17) leads to a particularly simple expression for the heat capacity of the sample C_s, if C_r is zero, *i.e.* if no empty pan is placed on the reference side of the MDSC ($C_r \approx 0$). The measured C_s is, as usual, the specific heat capacity of the sample, c_p multiplied with the mass m, plus the heat capacity of the empty pan, C'. The heat capacity of sample and pan is then:

$$C_s = mc_p + C' = \frac{KA_\Delta}{A_{T_s}\omega} \tag{18}$$

For the case of an empty (and identical pan to the sample pan) on the reference position, the calibration equation takes on the form:

$$mc_p = A_\Delta / A_{T_s}\sqrt{(K/\omega)^2 + C'^2} \tag{19}$$

i.e. in this case the overall calibration is not only dependent on the frequency of modulation, but also on the heat capacity of the empty reference pan.

Data treatment

In this section the treatment and deconvolution of the data generated by the MDSC is summarized as it applies to the present quasi-isothermal measurement ($q = 0$). The signal deconvolution is a running, real-time process that examines two cycles of input for each point generated as output. The output point is the

appropriately smoothed average at 1.5 cycles prior to the last measured point at t_3 (*i.e.* the data recording lags 1.5 cycles behind the measurement). For the better understanding of the calculation we define the relevant times for the generation of the last possible fully averaged and smoothed data point (at t_3) as follows:

t_0 = time of measurement of the last data point needed for the computation of the output for data at t_3. The output for the measured data at t_0 will only be ready at time $t_0+(3/2)p$

$t_1 = t_0-(1/2)p$ (with p = period of one cycle in s)

$t_2 = t_0-p$

$t_3 = t_0-(3/2)p$

$t_4 = t_0-2p$

At any time t, the average heat flow taken over the last full cycle of modulation is $<HF(t)>$. For equal positive and negative deviations, as in the heat flow due to the modulation only, this average should be zero. Using a non-zero heating rate q, or when experiencing a temperature drift of different frequency in the calorimeter $<HF(t)>$ is the total heat flow as would have been detected by standard DSC. At time t_1 the average heat flow is, for example:

$$<HF(t_1)> = \frac{\sum_{t_2}^{t_0} HF(t)}{n} = 0 \tag{20}$$

The heat flow is next deconvoluted by finding the in-phase and out-of-phase components as was discussed for T_s in Fig. 2 and Eq. (7):

$$HF_{\cos}(t) = [HF(t) - <HF(t)>]\cos \omega t \quad t \leq t_1 \tag{21}$$

$$HF_{\sin}(t) = [HF(t) - <HF(t)>]\sin \omega t \quad t \leq t_1 \tag{22}$$

The brackets in Eqs (21) and (22) represent the instantaneous amplitude of the oscillating heat flow at t corrected for any underlying heating rate q or drift [see also Fig. (2), replacing ε with δ and T_s with $HF = A_{HF} \sin(\omega t-\delta) = A_{HF}(\cos \delta \sin \omega t-\sin \delta \cos \omega t)$]. To obtain the amplitude A_{HF}, one averages (integrates) over one full period p. At t_2 this leads, for example to:

$$<HF_{\cos}(t_2)> = \frac{\sum_{t_3}^{t_1} HF_{\cos}(t)}{n} \quad [= (<A_{HF} / 2)\sin \delta>] \tag{23}$$

$$<HF_{sin}(t_2)> = \frac{\sum_{t_3}^{t_1} HF_{sin}(t)}{n} \quad [= (<A_{HF} / 2)\cos \delta>] \tag{24}$$

Simple vector addition of the two averages gives the average maximum amplitude of the heat flow due to modulation:

$$<A_{HF}(t_2)> = 2\sqrt{<HF_{sin}(t_2)>^2 + <HF_{cos}(t_2)>^2} \tag{25}$$

The average $<HF(t_3)>$ enters into the earliest limit of the summations of Eqs (23) and (24). It involves data starting from t_4 and shifts, thus, the beginning of the signal deconvolution to two cycles before t_0.

The deconvolution of the temperature amplitude as drawn in Fig. 2 is analogous to the heat flow deconvolution, so that only a listing of the corresponding definitions and equations is needed.

$<T_s(t)>$ = average sample temperature at t
$A_{T_s}(t)$ = peak of the temperature amplitude due to modulation at t
ε = phase lag of T_s in radians $[\theta(t) = \omega t - \varepsilon]$

$$<T_s(t_1)> = \frac{\sum_{t_2}^{t_0} T_s(t)}{n} \tag{26}$$

$$T_{cos}(t) = [T_s(t) - <T_s(t)>]\cos \omega t \quad t \le t_1 \tag{27}$$

$$T_{sin}(t) = [T_s(t) - <T_s(t)>]\sin \omega t \quad t \le t_1 \tag{28}$$

$$<T_{cos}(t_2)> = \frac{\sum_{t_3}^{t_1} T_{cos}(t)}{n} \quad [= <(A_{T_s} / 2)\sin \varepsilon>] \tag{29}$$

$$<T_{sin}(t_2)> = \frac{\sum_{t_3}^{t_1} T_{sin}(t)}{n} \quad [= <(A_{T_s} / 2)\cos \varepsilon>] \tag{30}$$

$$<A_{T_s}(t_2)> = 2\sqrt{<T_{sin}(t_2)>^2 + <T_{cos}(t_2)>^2} \tag{31}$$

The signals just calculated and averaged at temperature t_2 are further smoothed by computing the additional averages given next. The need for the smoothing causes a three half-cycle delay in recording of a data point at t_3 after measuring at t_0:

$$\text{smoothed} \quad \langle A_{HF}(t_3)\rangle = \frac{\sum_{t_4}^{t_2} \langle A_{HF}(t)\rangle}{n} \tag{32}$$

$$\text{smoothed} \quad \langle HF(t_3)\rangle = \frac{\sum_{t_4}^{t_2} \langle HF(t)\rangle}{n} \tag{33}$$

$$\text{smoothed} \quad \langle A_{T_s}(t_3)\rangle = \frac{\sum_{t_4}^{t_2} \langle A_{T_s}(t)\rangle}{n} \tag{34}$$

$$\text{smoothed} \quad \langle T_s(t_3)\rangle = \frac{\sum_{t_4}^{t_2} \langle T_s(t)\rangle}{n} \tag{35}$$

The heat capacity $C_p(t)$ is computed by using the smoothed values of the reversing amplitudes as suggested by Eq. (18):

$$C_p(t_3) = K' \times \frac{\text{smoothed} \langle A_{HF}(t_3)\rangle}{\text{smoothed} \langle A_T(t_3)\rangle} \times \frac{1}{\omega} \tag{36}$$

The constant K' is defined as the Newton's law constant whenever heat capacity is to be derived from heat flow HF instead of from ΔT (Eq. (6) for units).

Where applicable, all output signals are smoothed and generated at the earliest time possible relative to the measuring time t_0, namely at t_3:

Time	t_3	[s]

The nonreversing, smoothed values for:

Temperature	$\langle T_s(t_3)\rangle$	[K or °C]
Total heat flow	$\langle HF(t_3)\rangle$	[mW]

The computed (smoothed) output for:

Heat capacity	$C_p(t_3)$	[mJ/K]

The instantaneous values for the:

Modulated temp.	$T_s(t_3)$	[K or °C]
Modulated	$HF\ HF(t_3)$	[mW]

The smoothed values for the amplitudes:

T amplitude	$<A_{T_s}(t_3)>$	[K or °C]
HF amplitude	$<A_{HF}(t_3)>$	[mW]

All of these output signals were recorded in the present research and used for the discussion. Additional data, such as the reversing heat flow, the nonreversing heat flow and phase information are not needed for the present discussion since $q = 0$ and only the reversing signal is used for heat capacity measurement.

Experimental

Instrumentation

A commercial Thermal Analyst 2910 system from TA Instruments Inc. with modulated DSC (MDSC) was used for all measurements (Fig. 2). For the measurements above ambient temperature, dry N_2 gas with a flow rate of 10 ml/min was purged through the sample. Below ambient temperature the sample was flushed with dry N_2, and then the N_2 flow was stopped. Compressed air flow of 150 ml/min or cold nitrogen, generated from liquid nitrogen were used for cooling for the respective above and subambient measurements. Heat capacities were calibrated with a sapphire standard [18]. The temperature calibration was carried out using the onsets of the transition peaks for cyclohexane (186.1 and 279.7 K), naphthalene (353.42 K), indium (429.75 K) and tin (505.05 K). Sample masses were 5–30 mg except for sapphire (where up to 144 mg were used). The pan weights were always about 25 mg and matched on sample and reference sides.

Four kinds of experiments have been carried out: 1) the dependence of the calibration constant on oscillation frequency was checked under different conditions; 2) at a given temperature and fixed modulation period, the temperature amplitude was varied until it exceeded the actually maximum amplitude the in-

strument could achieve; 3) the heat capacity was measured at a given isothermal temperature for up to 20 minutes with fixed modulation period and temperature amplitude. Data of the last 10 minutes are reported as the measured C_p; 4) as an additional parameter the weight was varied as in the experiments of type 3. All available signals were recorded. The discussed signals are, as listed in the prior section.

Samples

The sapphire disc and indium for calibration were supplied with the accessory kit of the MDSC instrument. Aluminum and selenium pellets of 99.999% purity were obtained from Aldrich Chem. Co., Milwaukee, WI. Sodium chloride of analytical reagent grade was acquired from Mallinckrodt Co., Paris, KY. A standard sample of polystyrene of MW = 100,000, $M_W/M_n < 1.06$ was bought from Polyscience Inc., Warrington, PA. The quartz used in this work was pure, supplied by the University glass-blower in suitable shape.

Results

Figure 3 shows the maximum temperature amplitude the MDSC can reach at a given temperature with the period of oscillation of 60 seconds and the cooling conditions of 150 ml/min air flow through the DSC outside of the DSC cell (above ambient condition). Obviously, the higher the isothermal temperature, the higher the amplitude that can be reached. Considerably higher amplitudes are permissible with the mechanical or liquid nitrogen cooling accessory, as is shown in Fig. 4. To choose the experimental parameters, one is limited to temperature amplitudes below the values shown in the curve. If one plans, for example, to run an experiment from 320 to 470 K at a period of 60 s, the temperature amplitude must not be more than 0.3 K, as shown in Fig. 3. For different cooling conditions, similar plots should be made to be able to make the proper choice of frequency and amplitude.

Table 1 displays the calibration constant $K_c = C_p(\text{literature})/C_p(t_3)$ [Eq. (36)] for two temperature amplitudes A_{T_s} [Eq. (2)] and different period settings p at 320 K. Note, that for all experiments the factory-setting of 1.00 for the K_c was not changed, which results in values different from 1.00 for K_c. Clearly, there is, particularly at the high frequencies, a dependence of K_c on p, as expected from the discrepancy between Eqs (19) and (36). Only for the case of $C_r = 0$ [no reference pan, Eq. (18)] should K_c be independent of p. In this case one needs, however, to remember that C_s is the heat capacity of sample+pan ($mc_p + C'$). There is practically no dependence of K_c on the temperature

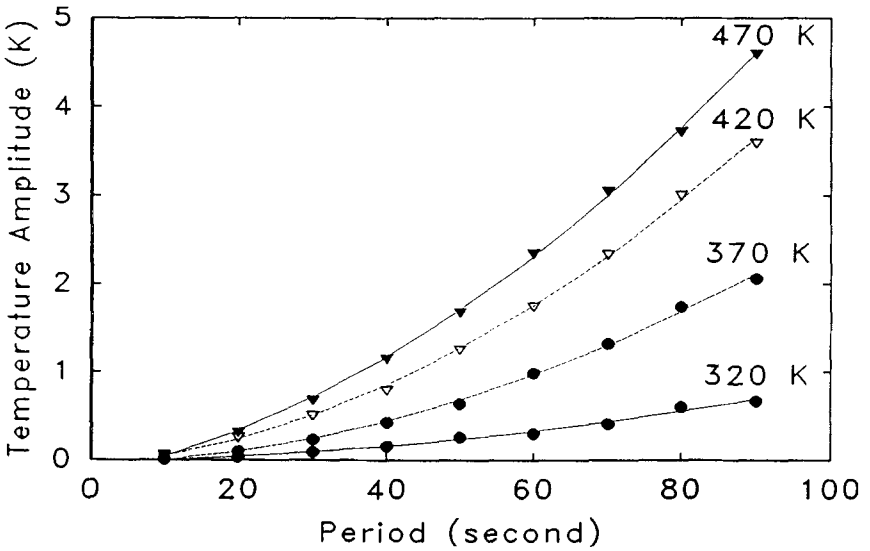

Fig. 3 Maximum amplitude of the sample temperature T_s (A_{T_s}) that can be reached for the given condition of cooling with air at ambient temperature

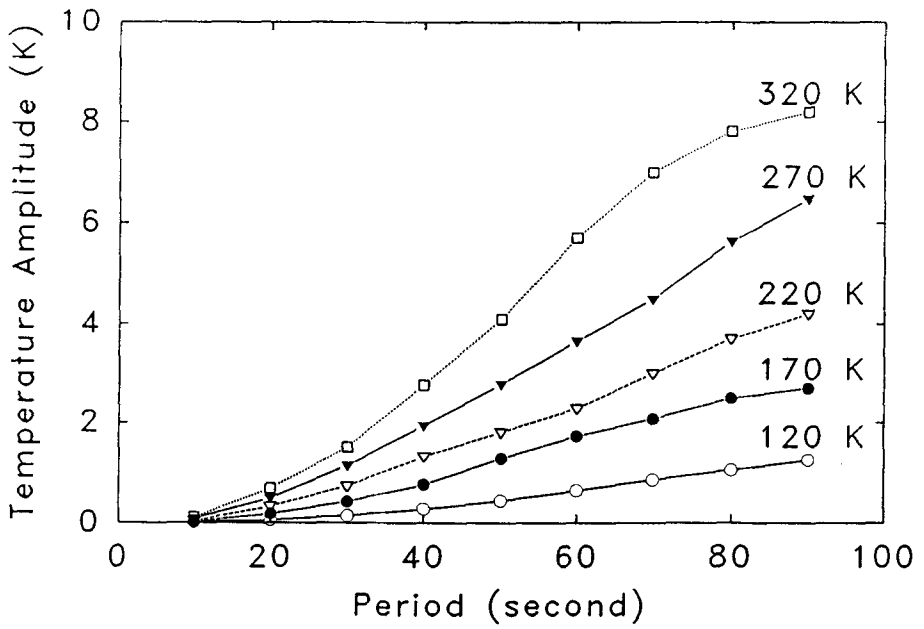

Fig. 4 Maximum amplitude of the sample temperature T_s (A_{T_s}) that can be reached for the given condition of cooling with liquid-N_2-generated nitrogen

amplitude, as expected from Eqs (17–19). Still, the smallest variation of K_c with p seems to occur at $p \approx 50$ s.

Figure 5 shows a series of actual heat capacity measurements [Eq. (36)] at a constant temperature (470 K) and period (60 s) and different temperature amplitudes A_{T_s}. The heat capacity (dashed line, top curve on the left, left scale) shows considerable noise until A_{T_x} exceeds several tenth of a kelvin or a heating rate of about 1 deg·min^{-1}. By increasing the temperature amplitude, one can improve the data precision significantly. Perhaps it is not surprising that maximum precision is reached for similar heating rates as used in conventional DSC. The limit of A_{T_s} is reached when the set value can not be reached, as given in Fig. 3 ($A_{T_s} \approx 2.5$ K under the conditions of Fig. 3).

Table 1 Effect of p and A_{T_s} on K_c

p/	K_c		Difference/
s	$A_{T_s} = 0.05$ K	$A_{T_s} = 0.2$ K	%
10	3.1521		
20	2.1234		
30	1.5746	1.5604	0.91
40	1.3234	1.3217	0.13
50	1.1955	1.1942	0.11
60	1.1268	1.1234	0.30
70	1.0892	1.0862	0.28
80	1.0601	1.0557	0.42
90	1.0438	1.0357	0.78

The C_p-calibration constant K_c, as evaluated in Table 1, is only approximately independent of temperature and its change with temperature needs to be established. Figure 6 shows this temperature dependence. Not only does it decrease slightly with temperature, but during the time of these experiments it had also a break between 400 and 440 K, which is consistent with results from other instruments and earlier reported data [8]. This break was caused by instrument factors (internal thermocouple calibration) and has been corrected in the meantime. A one-point calibration for the heat capacity constant, is (as in all other commercial heat capacity programs) not sufficient, and a full temperature dependence, as shown in Fig. 6 must be established if precision better than a few per cent is required.

The effect of sample mass on the heat capacity was studied with sapphire standards and the results are shown in Fig. 7. The higher sample mass causes a lower measured heat capacity, due to insufficient thermal diffusivity. Lower sample mass will not necessarily increase the experimental error, since one can

improve the instrument sensitivity by increasing the amplitude of temperature oscillation within the limits of Fig. 3.

Making the required corrections with temperature and optimizing the conditions of measurement, the average error from isothermal MDSC heat capacity measurement might be brought to levels as low as ±0.1%. Five standard samples have been measured as a first attempt to evaluate the MDSC under the constant temperatures conditions. The results are shown in Fig. 8 with average and RMS errors of −0.9±1.0%. These results can be further improved by optimizing sample mass, use of the Autosampler to place the sample and reference pans reproducibly, and choosing larger temperature amplitudes by increasing the cooling power.

Discussion

The MDSC brings a significant advance to calorimetry. Once the optimum operation conditions have been established (Figs 3, 4 and 7 and Table 1), precise measurement of heat capacity can be made by automatic, stepwise heating or cooling (Fig. 8). The highest precision is reached with maximum modulation (A_{T_s}), minimum period (p), and maximum sample heat capacity $C_s(= mc_p + C')$, all limited by the stringent condition of negligible temperature gradient within the sample and continued steady state [13, 14]. If the modulation cannot affect the full sample with the amplitude set for the analysis, one cannot expect quantitative data, as is illustrated in Fig. 7. If, on the other hand, the modula-

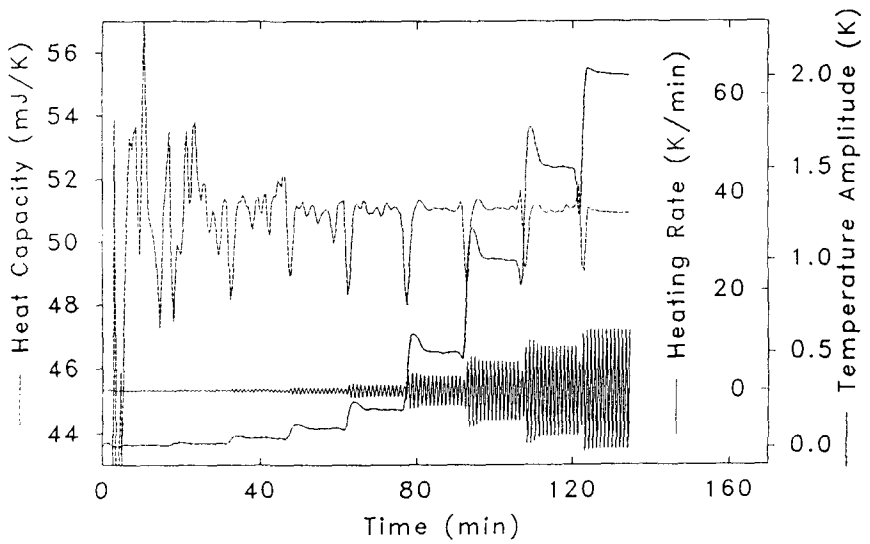

Fig. 5 Heat capacity of 62.54 mg of sapphire, heating rate, and temperature amplitude A_{T_s} as a function of time at T_0 = 470 K (p = 60 s or 0.0167 Hz)

tion is too low, precision suffers, as is illustrated on the left side of Fig. 6. It is also possible to measure under conditions of changing temperature ($q \neq 0$) and then quantitatively separate the reversible effect (measured by modulation) from the overall heat effect (measured by the total heat flow $\langle HF(t_3) \rangle$). A number of

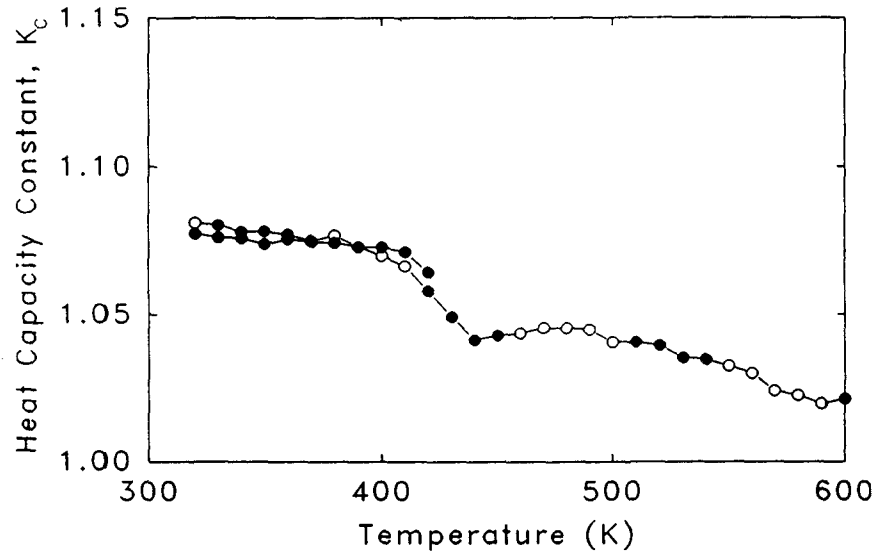

Fig. 6 Change of the heat capacity constant K_c as a function of temperature (p = 60 s, 62.54 mg sapphire, A_{T_s} = 0.2 K)

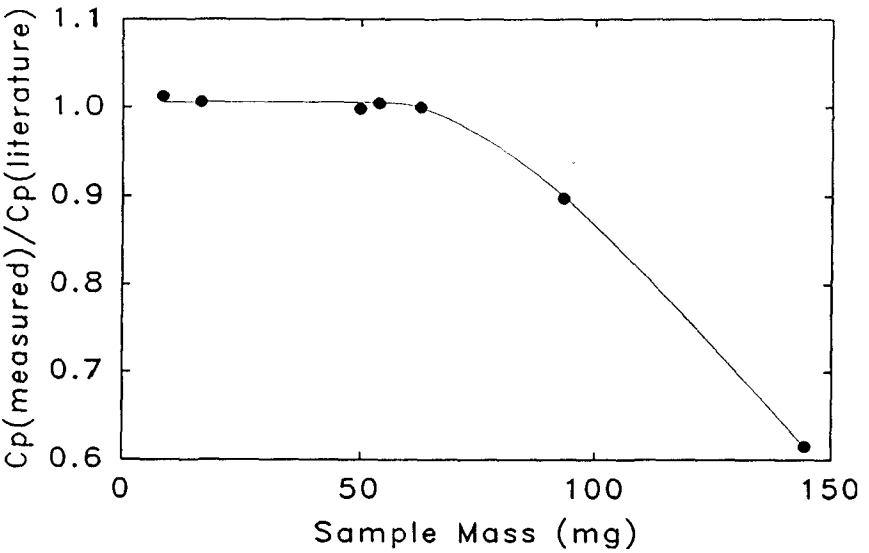

Fig. 7 Change of the measured heat capacity as a function of sample mass for a sapphire standard (p = 60 s, T_0 = 320 K, A_{T_s} = 0.2 K)

qualitative and quantitative applications are described in the literature [8, 10]. Since, especially in macromolecular materials, many processes are not fully reversible, many new applications are now open for quantitative differential thermal analysis.

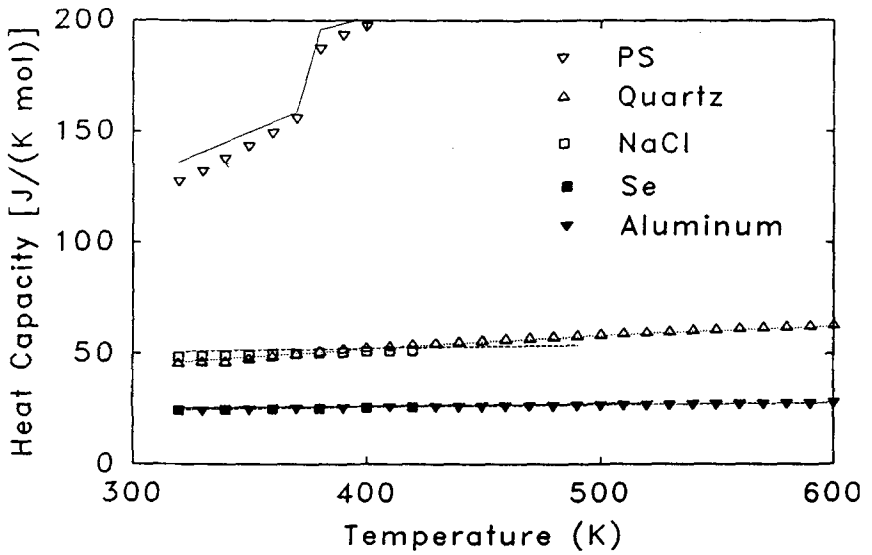

Fig. 8 Heat capacities of five standard samples. Symbols represent the experimental data; lines, reports from the literature (measuring conditions: p = 60 s, A_{T_s} = 0.2 K, PS: 9.576 mg, SiO_2: 16.20 mg, NaCl: 63.12 mg, Se: 122.7 mg, Al: 41.78 mg)

In the MDSC used, the sample-temperature amplitude A_{T_s} is a fixed parameter. It is set at the beginning of the run and the modulated heat-input at the block is adjusted to reach this condition (Fig. 1). Naturally, the thermal conductivity of sample and instrument must be such, that this goal can be achieved. The limits are illustrated in Figs 3 and 4. Similar plots should be available for the particular instrument for the given run conditions and sample type. Figure 5 is a typical example of satisfactorily chosen A_{T_s} over the full range of amplitudes (dash-dotted line, right-outer scale, lowest curve on the left, highest on the right). Due to the increase of precision, the highest A_{T_s} gives the most precise data. Note, that it takes two cycles (2 min for Fig. 5) until steady state can be observed after it has actually been reached because of the averaging and smoothing procedure [Eqs (20), (26) and (32–35)]. The steady state of modulated MDSC can be computed to be attained by a factor ω more slowly than for standard DSC, as shown by Eq. (4) of [9]. After additional cycles, the smoothed values reach their steady state.

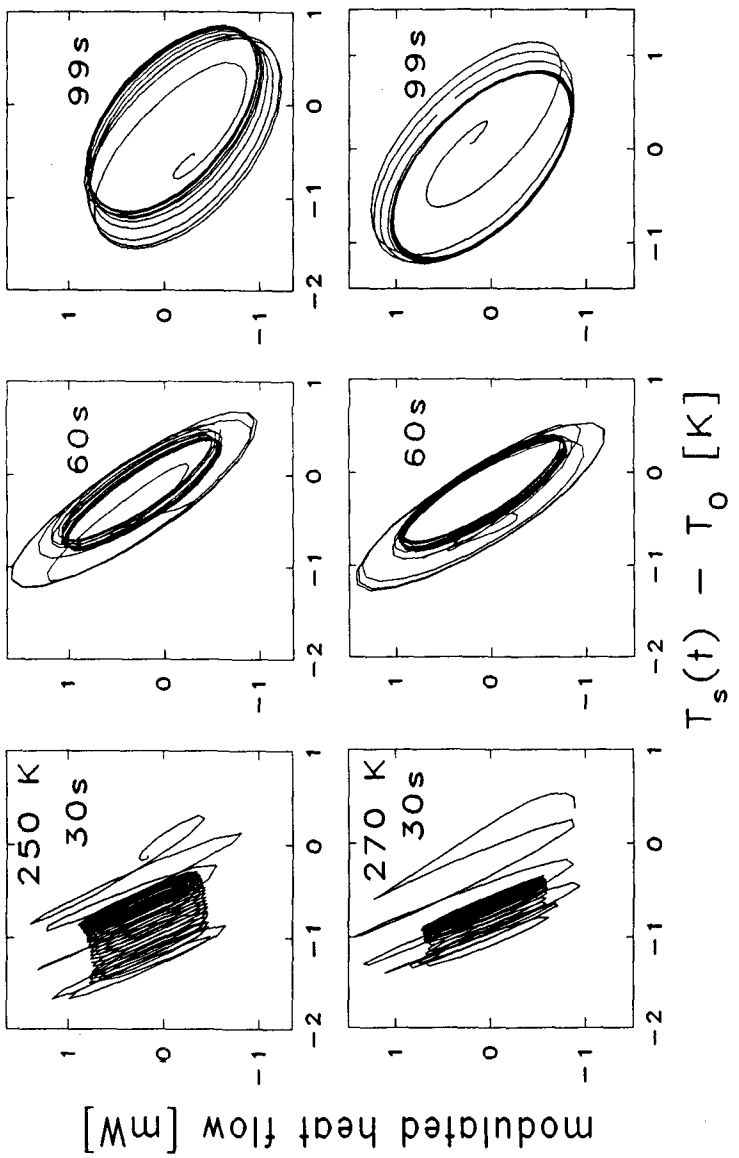

Fig. 9 Plot of $HF(t)$ *vs.* $T_s(t)$ for runs at 250 and 270 K using liquid-N_2-cooled nitrogen (24.90 mg of sapphire in the sample pan of 22.86 mg; empty reference pan of 22.91 mg; p = 30, 60 and 99 s left to right; A_{T_s} = 0.3, 0.6 and 1.0 K left to right, so that the heating rates in all three experiments are similar, see Fig. 4)

The continuous change in calibration constant K_c makes it necessary, as in any other heat capacity measurement, not to rely on a single-point calibration. As the temperature changes, the ratio of heat carried from block to sample and reference by conduction and radiation changes, making it impossible to construct an instrument with a constant K_c. Most important is, however, to establish the proper heat capacity calibration constant for the chosen period p. Equation (36) used by the MDSC software is correct only for the case of $C_r = 0$ (no reference pan). In this case, however, the measured heat capacity applies to $mc_p + C'$ [Eq. (18)].

As seen from Table 1 the calibration constant increases with frequency. Inserting $K_c = C_p$ (literature)/$C_p(t_3)$ into Eq. (36) and replacing the ratio of amplitudes by the proper expression derived from Eq. (19) leads to the following equation for the frequency dependence of the calibration constant K_c [note the substitution of A_{HF} for A_Δ in Eq. (19)]:

$$K_c = C_p(\text{literature})/mc_p \sqrt{1 + (C'\ \omega / K)^2} \tag{37}$$

An appropriate regression analysis of the data of column 2 of Table 1 leads to a value of 1.1±0.1 for C_p(literature)/mc_p ($R^2 = 0.98$). The smaller range of p in column 3 gives 0.8905 for the ratio with an R^2 of 0.999. Although Eq. (37) can be used to calculate K_c for any frequency, systematic deviations from the regression line, as well as the small dependence on A_{T_s} makes it more advisable to calibrate at the frequency of measurement, preferably at the prior evaluated minimum in A_{T_s} dependence (50 s in Table 1).

A general test of the quality of the state of the MDSC experiment can be obtained by plotting the instantaneous values for the modulated heat flow [$HF(t)$] *vs.* the modulated temperature [$T_s(t)$]. In Fig. 9 six examples are given, illustrating the approach to the steady state ellipse that results under ideal control and response of the MDSC from the two modulated signals with different phase lags [Eqs (7) and (8) for T_s and (9) and (11) for $T_r - T_s = \Delta T$, the latter can be changed to HF by remembering that $\Delta T = HF \times K'/K$]. Once steady state is reached, the same figure is traced. The small drifts in sample temperatures would not affect the quality of the measurement since only the maximum amplitudes are extracted for the heat capacity evaluation [Eqs (25) and (31)]. The ellipses should be centered about zero heat flow and at the set-point temperature (T_0). Deviations express the asymmetry of the instrumental set-up. The best performance comes, thus, from the data at 60 s (center figures).

Figure 10 illustrates some cases of larger temperature and heat flow drifts during the measurement on the example of an empty sample and reference pan. As long as the ellipse is shifted as a whole, such drifts will, again, only result in minimally effects on the MDSC data. In case of nonzero q these drifts would

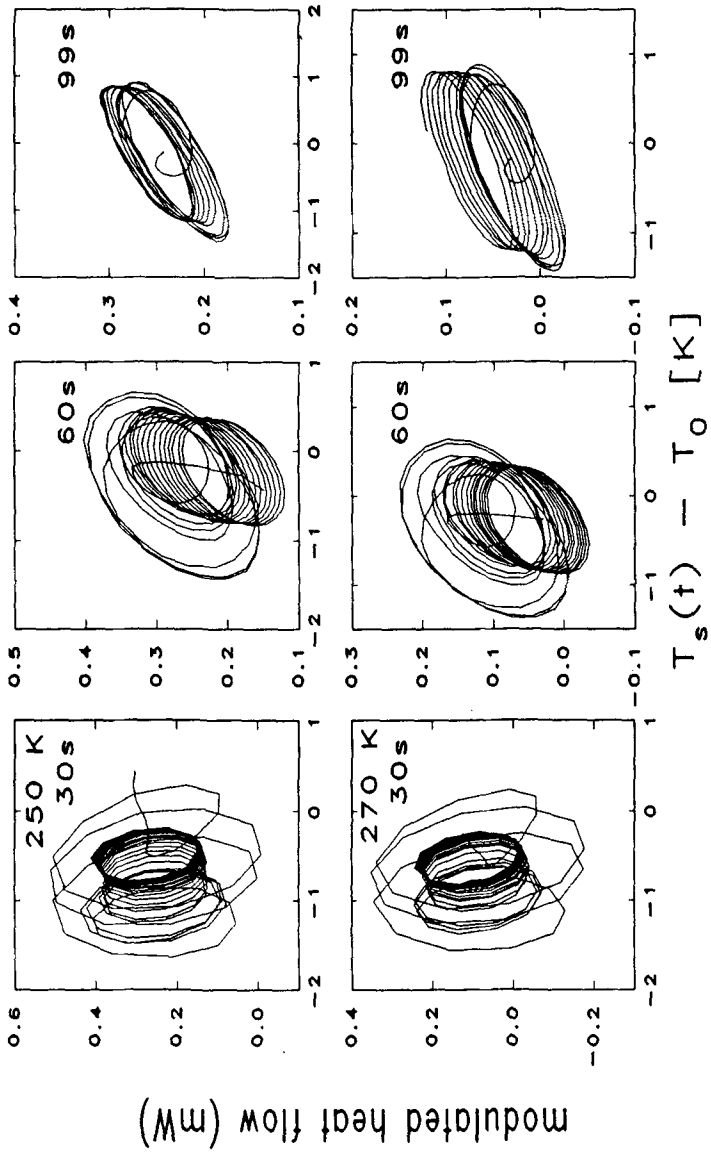

Fig. 10 Plot of $HF(t)$ *vs.* $T_s(t)$ for runs at 250 and 270 K using liquid-N_2-cooled nitrogen (empty sample pan of 22.89 mg; empty reference pan of 22.91 mg;other conditions as in Fig. 9)

distort the overall heat flow and lead to considerable error in measurement. While a standard DSC has no means to recover data under such conditions, MDSC still can produce acceptable, quantitative results.

Figure 11 shows a more serious distortions of the ellipse due to insufficient cooling capacity for the chosen run parameters. Note that the operation conditions put this run at the limits of Fig. 3 (air cooling at relatively low T_0). The right-hand-side of the ellipse represents the cooling segment of the modulation that is poorly controlled. The left-hand-side, representing the heating segment, in contrast has little difficulty. Due to the extensive averaging on data treatment, useable data can still be derived, as long as the average maximum amplitudes remain unchanged. Naturally, performances of this type should be avoided. Plots of this type permit one to eliminate much of the guessing why a particular run may not have given reliable results and point to the reasons for failure. They also point out the various drifts and asymmetries. An early example from our laboratory showed that it was possible, for example, to measure the heat capacity of fullerenes far into the temperature range of oxidation [19]. The enthalpy of reaction was much bigger than the heat capacity effect and caused an enormous drift, but since it did not contain any modulation it was quantitatively eliminated in the MDSC.

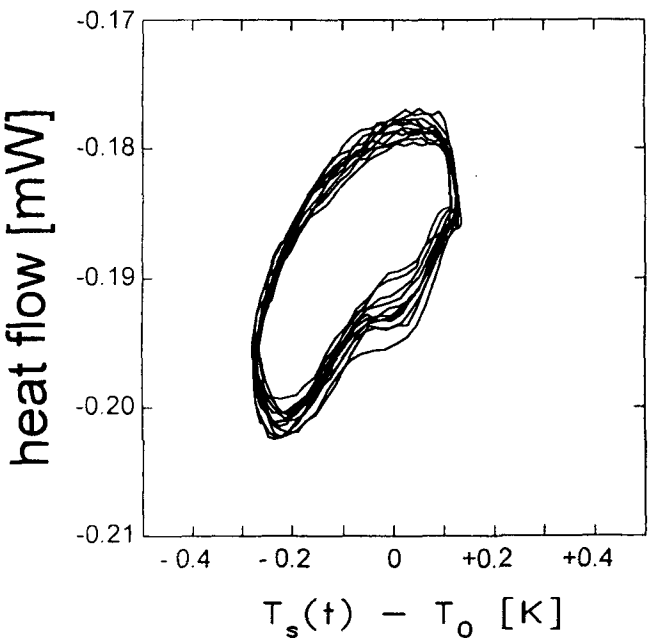

Fig. 11 Plot of $HF(t)$ *vs.* $T_s(t)$ for a run at 320 K using only air cooling (empty sample and reference pans of 22.82 mg; p = 60 s, A_{T_s} = 0.2, see Fig. 3)

Conclusions

Using MDSC, it is possible to measure heat capacity in close to thermal and internal equilibrium with a precision better than in standard DSC. Especially samples that suffer from irreversible effects on fast temperature changes during measurement should be measured in this fashion. The 'quasi-isothermal' measurement allows, furthermore, to establish conditions for optimal operation of the instrument and gives easy diagnostic information. The correction for standard DSC caused by differences in sample and reference heating rates is eliminated. Full tables of heat capacities at fixed (usually 10 K) intervals can be generated by properly programming automatic measurement and computation. Adding a constant heating rate q permits simultaneous recording of the standard overall DSC heat flow (with all its sample- and instrument-caused irreversible effects) and the reversing heat flow. A separation of the two signals allows further insight into materials behavior, as will be shown in future publications. With this study of MDSC we hope to have given an answer to the recently raised questions: who needs MDSC? and what is it good for?

* * *

This work was supported by the Division of Materials Research, National Science Foundation, Polymers Program, Grant # DMR 92-00520 and the Division of Materials Sciences, Office of Basic Energy Sciences, U.S. Department of Energy, under Contract DE-AC05-84OR21400 with Martin Marietta Energy Systems, Inc.

The authors acknowledge several helpful discussions of the part on data treatment by Drs. P. S. Gill, B. S. Crowe and S. R. Sauerbrunn of TA Instruments, M. Reading of ICI, and of the part on derivation of the equations for quasi-isothermal heat capacity measurement by Dr. R. Gunther of the University of Nebraska. Instrumentation was made possible by a loan of TA Instruments.

References

1 A. Mehta, R. C. Bopp, U. Gaur and B. Wunderlich, J. Thermal Anal., 13 (1987) 197.
2 B. Wunderlich and U. Gaur, ACS Adv. in Chemistry, Series 203, C. D. Craver, ed. Washington DC, p. 195, 1982.
3 U. Gaur, A. Mehta and B. Wunderlich, J. Thermal Anal., 13 (1978) 71; A. Mehta and B. Wunderlich, Coatings and Plastics Preprints, Am. Chem. Soc., 35 (1975) 393.
4 B. Wunderlich, J. Thermal Anal., 32 (1987) 1949.
5–7 Y. Jin and B. Wunderlich, J. Thermal Anal., 36 (1990) 365; 1519; and 38 (1992) 2257.
8 S. R. Sauerbrunn , B. S. Crowe and M. Reading, 21st Proc. NATAS Conf. in Atlanta GA, Sept. 13–16, pp. 137–144 (1992); M. Reading, B. K. Hahn, and G. S. Crowe, US Patent 5,224,775 (July 6, 1993).
9 B. Wunderlich, Y. Jin and A. Boller, Thermochim. Acta, to be published (1994).

10 M. Reading, D. Elliot and V. L. Hill, J. Thermal Anal., 40 (1993) 949; P. S. Gill, S. R. Sauerbrunn and M. Reading, J. Thermal Anal., 40 (1993) 931; M. Reading, Trends in Polymer Sci., 8 (1993) 248.
11 P. F. Sullivan and G. Seidel, Phys. Rev., 173 (1968) 679.
12 G. Dixon, S. G. Black, C. T. Butler and A. K. Jain, Anal. Biochem., 121 (1982) 55.
13 B. Wunderlich, 'Differential Thermal Analysis, A. Weissberger and B. W. Rossiter eds. 'Physical Methods in Chemistry.' Vol. 1, Part V, Chapter 8. J. Wiley and Sons, New York, 1971.
14 B. Wunderlich, 'Thermal Analysis,' Academic Press, Boston, MA 1990.
15 W. Hemminger and G. Höhne, 'Calorimetry,' Verlag Chemie, Weinheim, 1984.
16 J. M. Sturtevant, 'Calorimetry,' in A. Weissberger and B. W. Rossiter eds. 'Physical Methods in Chemistry.' Vol. 1, Part V, Chapter 7. J. Wiley and Sons, New York, 1971.
17 A. Boller, C. Schick and B. Wunderlich, to be submitted 1994.
18 D. A. Ditmars, S. Ishihara, S. S. Chang, G. Bernstein and E. D. West, J. Research, Natl. Bur. Stand., 87 (1982) 159.
19 Y. Jin, A. Xenopoulos, J. Cheng, W. Chen, B. Wunderlich, M. Diack, C. Jin, R. L. Hettich, R. N. Compton and G. Guiochon, Mol. Cryst. Liq. Cryst., to be submitted 1994.

Zusammenfassung — Die mathematischen Gleichungen für die stufenweise Messung der Wärmekapazität (C_p) mit modulierter Differential kalorimetrie (MDSC) werden für die Bedingung eines vernachlässigbar kleinen Temperaturgradierten in Probe und Referenzsubstanz diskutiert. Diese neue Technik ermöglicht die Bestimmung von C_p ohne die Probe wesentlich vom Gleichgewicht zu entfernen, eine Bedingung die conventionelles DSC nicht erreichen kann. Die Wärmekapazität is unter "praktisch isothermer Bedingung" gemessen worden (haäfig innerhalb ±1 K). Diese Methode gibt Daten von guter Qualität. Die Effekte der Probenmasse, Amplitude und Frequenz der Temperaturmodulation wurden untersucht und Methoden für die Optimirung des Instruments werden vorgeschlagen. Die Korrekturen für Unterschiede zwischen Proben- und Refernztemparatur aufheizgeschwindigkeiten die für das normale DSC fü Daten von hoher Qualität gebraucht werden, sind für diese Methode nicht nötig.

PROFESSOR BERNHARD WUNDERLICH IS RECIPIENT OF THE 1993 STK 'APPLIED CHEMICAL THERMODYNAMICS' AWARD

Bernhard Wunderlich, Professor of Chemistry at the University of Tennessee, Knoxville and ORNL/UT Distinguished Scientist, was honored by the Swiss Society of Thermal Analysis and Calorimetry (STK) on September 13, 1993 at the GEFTA/STK Thermal Analysis Symposium in Neuherberg, Germany.

The Swiss Society presented this prestigious award to Prof. Wunderlich in recognition of his innovative and comprehensive research on the thermodynamic characterization of solid state macromolecules. The Award Certificate cites his prominent books, his more than 350 papers published in distinguished scientific journals, and lists some of his most significant achievements during his tenure at Cornell University (1958–1963), at the Rensselaer Polytechnic Institute (1963–1988), and since 1988 at the University of Tennessee and the Oak Ridge National Laboratory. Among others, he is given a tribute for creating the Advanced THermal AnalysiS (ATHAS) Laboratory where he and his students established a unique data bank of critically evaluated thermodynamic properties (heat capacity, enthalpy, entropy) for polymers and related small molecules.

From the Editor:

A very active member of our Advisory Board since its inception, Professor Wunderlich made invaluable contributions to establishing and maintaining the high level of the J.Thermal Anal. by critically reviewing innumerable research papers. Throughout the 25-year lifespan of this Journal, he made himself always available for advice and guidance. The Editors of the Journal of Thermal Analysis, and the Members of it s Editorial Advisory Board extend their warmest congratulations to Professor Bernard Wunderlich for receiving the '1993 Applied Chemical Thermodynamics' Award from the Swiss Society of Thermal Analysis and Calorimetry.

J. Simon